Prostate cancer radiotherapy: potential applications of metal nanoparticles for imaging and therapy

Coulter, J. A., Butterworth, K. T., & Jain, S. (2015). Prostate cancer radiotherapy: potential applications of metal nanoparticles for imaging and therapy. *British Journal of Radiology*, *88*(1054), [20150256]. https://doi.org/10.1259/bjr.20150256

Published in:
British Journal of Radiology

Document Version:
Publisher's PDF, also known as Version of record

BJR

Received: 25 March 2015 | Revised: 1 June 2015 | Accepted: 4 June 2015

doi: 10.1259/bjr.20150256

Cite this article as:
Coulter JA, Butterworth KT, Jain S. Prostate cancer radiotherapy: potential applications of metal nanoparticles for imaging and therapy. *Br J Radiol* 2015; **88**: 20150256.

NANOPARTICLES FOR DIAGNOSTIC IMAGING AND RADIOTHERAPY SPECIAL FEATURE: REVIEW ARTICLE

Prostate cancer radiotherapy: potential applications of metal nanoparticles for imaging and therapy

[1]J A COULTER, PhD, [2]K T BUTTERWORTH, PhD and [2]S JAIN, MB BCh, PhD

[1]School of Pharmacy, McClay Research Centre, Queen's University Belfast, Belfast, UK
[2]Centre for Cancer Research and Cell Biology, Queen's University Belfast, Belfast, UK

Address correspondence to: Dr Suneil Jain
E-mail: *s.jain@qub.ac.uk*

ABSTRACT

Prostate cancer (CaP) is the most commonly diagnosed cancer in males. There have been dramatic technical advances in radiotherapy delivery, enabling higher doses of radiotherapy to primary cancer, involved lymph nodes and oligometastases with acceptable normal tissue toxicity. Despite this, many patients relapse following primary radical therapy, and novel treatment approaches are required. Metal nanoparticles are agents that promise to improve diagnostic imaging and image-guided radiotherapy and to selectively enhance radiotherapy effectiveness in CaP. We summarize current radiotherapy treatment approaches for CaP and consider pre-clinical and clinical evidence for metal nanoparticles in this condition.

Prostate cancer (CaP) is the most commonly diagnosed cancer in males and is responsible for more than 10,000 deaths each year in the UK.[1] Technical advances in radiotherapy delivery, including image-guided intensity-modulated radiotherapy (IG-IMRT), have enabled the delivery of higher radiation dose to the prostate, which has led to improved biochemical control. Further improvements in cancer imaging during radiotherapy are being developed with the advent of MRI simulators and MRI linear accelerators.[2–4]

Nanotechnology promises to deliver significant advancements across numerous disciplines.[5] The widest scope of applications are from the biomedical field including exogenous gene/drug delivery systems, advanced biosensors, targeted contrast agents for diagnostic applications and as direct therapeutic agents used in combination with existing treatment modalities.[6–11] This diversity of application is especially evident within cancer research, with a myriad of experimental anticancer strategies currently under investigation.

This review will focus specifically on the potential of metal-based nanoparticles to augment the efficacy of radiotherapy in CaP, a disease where radiotherapy constitutes a major curative treatment modality.[12] Furthermore, we will also address the clinical state of the art for CaP radiotherapy and consider how these treatments could be best combined with nanotherapeutics to improve cancer outcomes.

CURRENT STATE OF THE ART IN PROSTATE CANCER DIAGNOSIS AND TREATMENT

The management of CaP is changing rapidly with advances occurring in diagnosis, imaging and treatment. Most males present with localized rather than advanced CaP at diagnosis. Current stratification methods place patients into low-, intermediate- and high-risk prognostic categories based on prostate-specific antigen levels, local staging and Gleason score.[13]

Males with low-risk CaP are increasingly managed with active surveillance, with large studies reporting 10-year cancer-specific survival rates of >98% with this management approach.[14] In this cohort, 75.6% of males were treatment free after 5 years of active surveillance.[15] The role of multiparametric MRI in active surveillance has been defined, and nanotechnology offers the potential for better imaging biomarkers to monitor patterns of disease.[16,17] The role of superparamagnetic iron oxide nanoparticles (SPIONs) in MRI nodal staging for CaP has previously been demonstrated.[18]

Intermediate CaP is a heterogeneous group, where treatment options include active surveillance, radical prostatectomy, external beam radiotherapy (EBRT), brachytherapy (BT) alone or in combination with androgen deprivation therapy (ADT) and/or EBRT. Randomized controlled trials of dose-escalated EBRT, with doses of 74.0–79.2 Gy in conventional

(1.8–2 Gy) fractions, have demonstrated 5-year biochemical progression-free survival of 64–80.4%.[19–22] These studies have demonstrated improved biochemical control compared with lower doses of EBRT at the expense of higher rates of bowel and urinary toxicity. EBRT requires linear accelerators capable of producing photon energy spectrums commonly peaking at 6 or 10 MV to deliver an adequate radiation dose to the prostate gland, which is situated centrally within the pelvis. Pre-clinical studies have suggested that metal nanoparticle sensitization occurs even at megavoltage (MV) energies, where Compton effects dominate.[11,23]

BT is radiotherapy using sealed radioactive sources placed next to the skin, inserted into a body cavity or, through needles, into tissues (interstitial BT).[24] There are compelling reasons for utilizing metal nanoparticles with kilovoltage (kV) photon energies where the photoelectric effect is dominant [energy deposited $\propto$ atomic number^4 (Z^4)], a concept supported by several theoretical studies (Figure 1).[25,26] BT commonly utilizes kV radiation sources, for example iodine-125 (^{125}I; 35.5 keV γ-rays, $t_{½}$ 30 days), and has been shown to result in excellent biochemical control rates of 75–98% at 5 years.[27] The direct placement of permanent radioactive sources into the prostate gland increases conformality of treatment compared with EBRT, resulting in enabling delivery of higher doses of radiation to the prostate with acceptable normal tissue toxicity. High-dose-rate (HDR) BT is commonly combined with EBRT in patients with unfavourable intermediate risk CaP (Gleason 4+3, >50% positive cores). An iridium-192 (205–612 keV γ-rays, $t_{½}$ 74 days) source is commonly used for treatment. With this approach, a single 15-Gy treatment of HDR BT was combined with 37.5 Gy in 15 fractions of EBRT resulting in 97% of patients becoming disease free at 5 years.[28]

Radiobiological studies suggest that CaP may have a lower α/β ratio than surrounding normal tissues, making it more sensitive to high dose-per-fraction radiotherapy.[29] An alternative method of biological dose enhancement is hypofractionation, which exploits the low α/β ratio observed in CaP. Recent technological advances have enabled the development of stereotactic ablative radiotherapy (SABR). Clinical studies of SABR have demonstrated excellent biochemical control rates with acceptable treatment-related toxicity.[30] Longer follow-up of existing studies is required and Phase III clinical trials are under way.[31] If radical CaP treatments of five fractions or less are demonstrated to have efficacy equal to or better than conventional radiotherapy, then the use of radiosensitizing nanoparticles, delivered intravenously or intratumorally, becomes feasible with a reduced likelihood of off-target effects from multiple administrations.

In patients with high-risk localized CaP, a combination of radiotherapeutic and systemic therapies is generally utilized to optimize cancer control. A landmark study demonstrated that the addition of ADT to EBRT improved 5-year overall survival from 62% in patients treated with EBRT alone to 78% in patients treated with combined therapy.[32] Similarly, more recent trials demonstrated the combination of EBRT with ADT improved overall survival when compared with ADT alone.[33] Nanoparticles are being widely investigated as drug carriers to enhance the effectiveness of systemic therapy with some agents in early-phase clinical trials.[34]

Radiotherapeutic advances in metastatic CaP have paralleled those in localized disease. Technological advances have enabled the development of SABR for areas of oligometastatic disease, delivering radical doses of radiation in a small number of

Figure 1. Schematic representation of radiation interactions when an incident photon interacts with a high atomic number (Z) material and their downstream applications in radiotherapy. (a) Compton scattering occurs when an incident photon is scattered by a weakly bound outer-shell electron causing the photon to be deflected and lose energy, which is then transferred to the electron that is ejected from the atom. (b) Photoelectric ionization occurs when an incident photon is fully absorbed by an inner-shell electron, transferring its energy to it and causing it to be ejected from the atom. (c) Outer-shell electrons can fall into this vacancy, liberating further energy, often in the form of additional secondary Auger electrons.

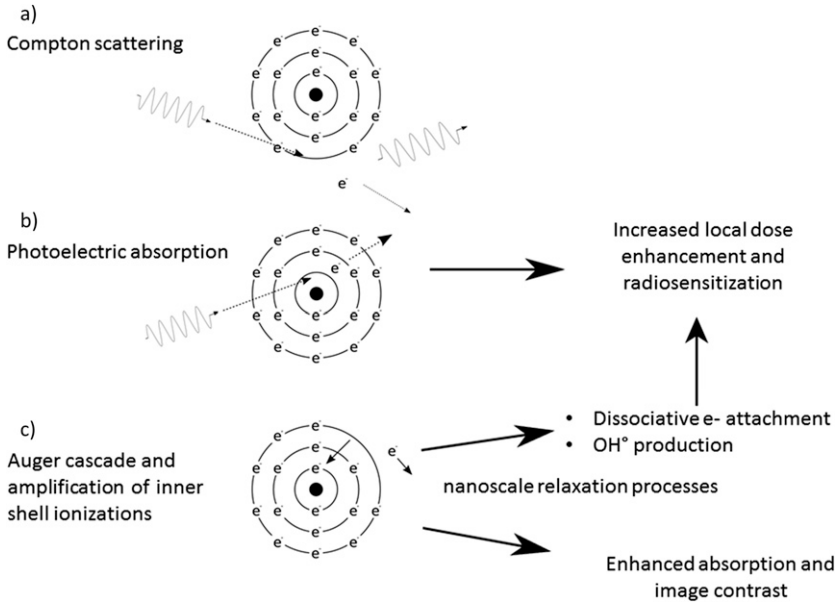

treatment fractions.[35] The α-emitter radionuclide radium-223 has been shown to prolong survival compared with the best supportive care (14.9 *vs* 11.3 months; HR, 0.70; $p = 0.002$) in patients with metastatic castrate-resistant CaP.[36] This systemic treatment is administered intravenously, accumulating at sites of bony metastatic disease and delivering highly damaging low-range α particles to these sites. Multifunctional nanoparticles utilized as drug delivery agents could enhance the specificity and effects of current systemic therapies used in CaP.

Although IG-IMRT has reached unprecedented levels of accuracy, there is significant potential for further improvement of radiotherapy delivery with the use of MRI. MRI simulation has a number of benefits over computerized tomography for treatment planning, enabling dose estimation in deformable soft tissues. It is likely that dose-painting and adaptive radiotherapy approaches will become the standard of care in the near future. International efforts are ongoing to develop an MRI-linac system for online, real-time soft-tissue image guidance.[2–4] Multifunctional gadolinium (Gd)-based agents that can be used for image contrast and radiation enhancement have significant potential to deliver innovative approaches in radiation oncology that may translate to human health gains.

METAL NANOPARTICLES

With the chemistry for metal nanoparticle synthesis well established, the ultimate choice of the core material depends largely on the downstream application. Attributes vary depending upon the composition of the core material but typically include superior biocompatibility relative to many existing pharmaceutical agents, tunability of nanoparticle size, shape and charge during the synthesis procedure and the relative ease with which additional functional groups can be conjugated to the surface.[37] Examples of functionalized nanoparticles are shown in Figure 2.

Iron-based nanoparticles

SPION, when adequately stabilized with organic surface coatings, can be homogeneously dispersed in suspensions known as ferrofluids. Following systemic administration, these colloid suspensions interact with external magnetic fields for imaging or, in some instances, to actively recruit nanoparticles to specific locations.[41] Early preparations of SPION were used as reticuloendothelial system MRI contrast agents that produce local inhomogeneities in the magnetic field during imaging. MRI contrast efficacy is established by reducing transverse relaxation (T2), where the rate of proton relaxivity is proportional to the iron atom concentration, thus providing negative contrast in MR images. While the

Figure 2. A schematic represention of a bi-functionalized, polyethylene glycol (PEG) stabilized gold-based nanoparticle (AuNP) including a variety of prostate cancer-specific active targeting moieties. NHS, *N*-hydroxysuccinimide.[9,38–40]

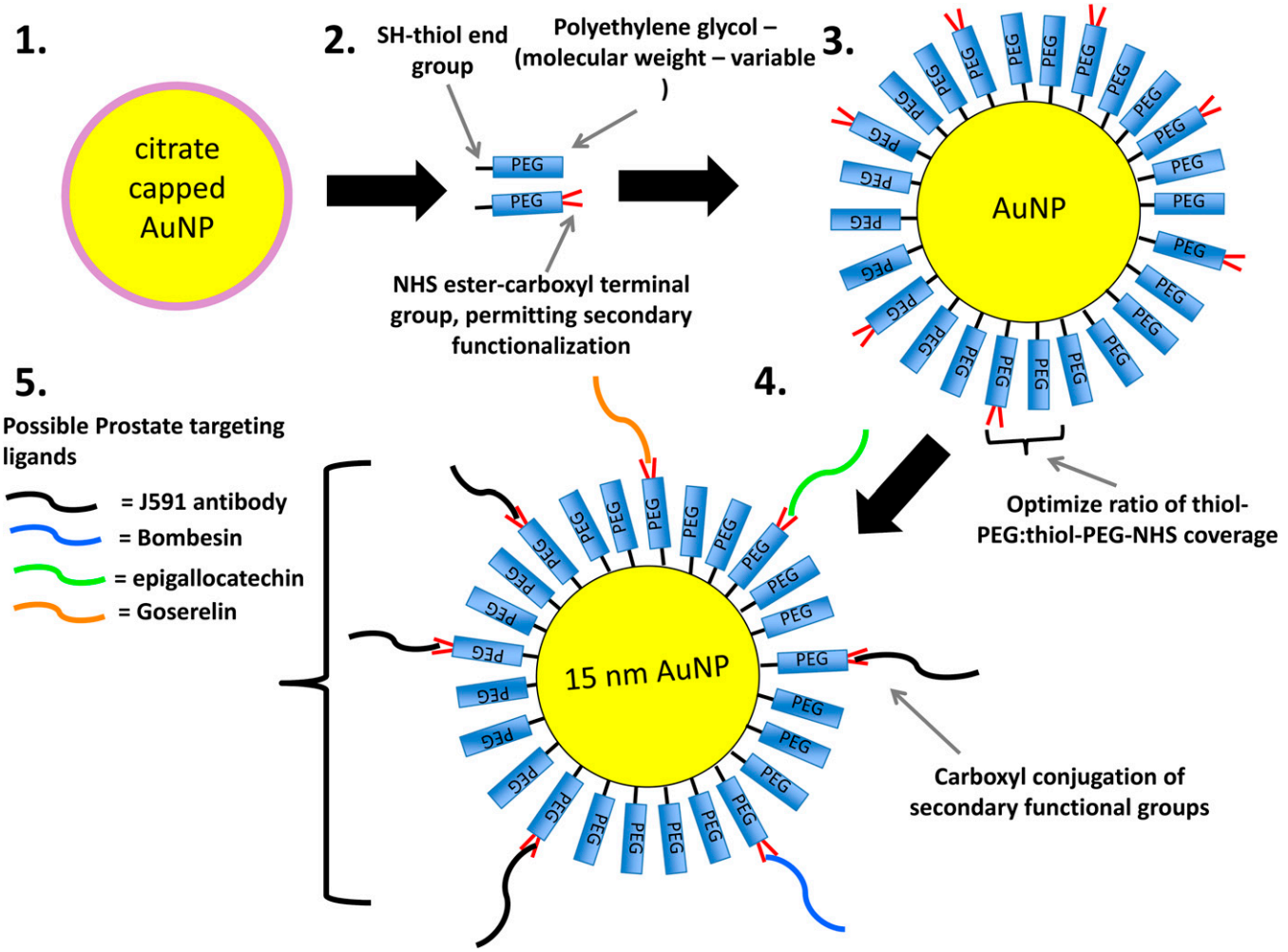

enhanced imaging capabilities of these preparations are clearly evident in the highly phagocytic environment of the liver, spleen and bone marrow, their application is limited with respect to the ultrasensitive detection of CaP for both localized disease and more specifically micrometastasis. To address this, several iron oxide nanoparticle (ION) preparations have been functionalized with CaP-targeting ligands with the aim of elevating intratumoral nanoparticle accumulation. Prostate-specific membrane antigen (PSMA) is a valid target for specific CaP targeting.[42] While normal prostate epithelium tissue expresses alternative cytosolic splice variants of PSMA, the transmembrane form is significantly elevated levels in CaP tissue, and has been shown to increase with Gleason grade.[43] Importantly, this mechanism for CaP tumour selectivity is not restricted to the primary tumour, with lymph node and bone metastatic deposits in the castrate-resistant setting also exhibiting elevated PSMA expression.[38,44] Tse et al[45] have recently developed an antibody (J591)–iron oxide conjugate designed to target an extracellular epitope of PSMA, with the aim of developing a superior CaP-MRI contrast agent. The specific targeting efficacy of J591 was well established from earlier radiolabelled J591 studies.[46,47] The focus of the present study was to determine that antibody conjugation did not impair targeting efficacy, along with demonstrating improved tumour-specific MRI contrast and minimal cytotoxicity. Using an orthotopic LNCaP (PSMA-expressing) xenograft model, the authors reported strong negative contrast following intravenous (i.v.) injection of J591-IONs at a concentration of 6 mg kg^{-1} within 2 h. Furthermore, nanoparticles were retained within the tumour for at least 24 h of administration; effects that were not achieved using stabilized, untargeted control preparations. This pre-clinical study clearly demonstrates the advantage of active targeting approaches rather than depending on passive accumulation owing to the enhanced permeability and retention (EPR) effect. However, it should be noted that significant quantities of both passive and targeted nanoparticles were observed post-mortem within the spleen, indicating that stealth strategies could be further optimized to increase circulation time and, as a direct consequence, tumour loading.

PSMA-targeted IONs as thermal therapy agents have also been recently reported. Using an alternative chemical synthesis procedure, bionized nanoferrite clusters were stabilized using polyethylene glycol (PEG) and targeted with a pre-validated small molecule inhibitor of PSMA.[48,49] In this study, the authors developed isogenic PC3-PSMA-positive and negative subcutaneous xenograft tumour models, reporting PSMA-positive tumour accumulation within 2 h of administration, with maximum intratumoral concentrations achieved 48 h post-injection.[49] Central to their therapeutic efficacy was the formation of nanoclusters yielding enhanced heat production owing to various magnetodynamic processes (hysteresis, Néel switching and frictional contributions).[50] Previously, exposure of clustered magnetic nanoparticles to an alternating magnetic field at a fixed frequency of 150 kHz facilitated near-complete regression of MTG-B murine breast xenograft models by producing intratumoral temperatures up to 55°C.[51] Therefore, applying this approach to a PSMA-expressing CaP is hypothesized to confer significant therapeutic benefit.[49] However, despite improved targeting efficacy, only 4.3 ± 0.4% of the injected dose per gram of tissue accrued within the tumour. This raises questions over the clinical applicability of this strategy, specifically with reference to limiting heat production and conductance beyond the target volume. Off-target effects were observed when nanoclusters generated rectal temperatures in excess of 41.5°C, with continued heat production after the shut down of the alternating magnetic field owing to conductance.[51,52] Clearly, further refinement is required before early-phase clinical trials can begin.

Iron possesses a relatively low atomic number ($Z = 26$), unlike metals with higher atomic numbers such as Gd ($Z = 64$), platinum ($Z = 78$) and gold (Au; $Z = 79$); as such, the magnitude of the mass absorption coefficient and subsequent amplification of radiation effects (radiosensitization) is expected to be limited. Despite this, several authors have reported significant *in vitro* CaP radiosensitization using both kV and MV X-ray sources.[53,54] Cross-linked dextran-coated IONs were avidly endocytosed by both HeLa and EMT-6 cells, producing a maximum reduction in cell viability of 18% following 48 h of coculture with the nanoparticles. The significance of this relatively low-toxicity profile is further heightened when considering the radiosensitization potential, generating mean radiation dose enhancement factors (DEFs) of 1.43 and 1.36 in HeLa and EMT-6 cells, respectively. Subsequently, Khoei et al[54] reported DEFs of 1.22 following megavoltage irradiation in DU145 CaP cells *in vitro,* using a chemically analogous nanoparticle. This provided proof-of-concept data that nanoparticles with an iron oxide core could potentially prove beneficial using clinically applicable radiation sources, while limiting the off-target effects associated with hyperthermia. Licensed clinical examples of such preparations that include Feridex and Resovist are already in clinical use as contrast agents.[55,56]

Gadolinium-based nanoparticles

Current MRI techniques rely on the i.v. injection of a paramagnetic contrast agent most commonly based on Gd chelates, as Gd has even unpaired electrons and a relatively long relaxation time. Most of these agents are Gd chelates, such as Gd-diethylenetriaminepenta-acetate (Gd-DTPA), which are non-diffusible blood pool tracers captured soon after bolus injection by haemodynamic signals depending on proton relaxation times and then transformed to an MR signal.[57,58]

In addition to the paramagnetic features of Gd ions, their relatively high atomic number suggests they may offer additional advantages as radiosensitizers at MV energies. In terms of the development of Gd-based nanoparticle platforms for improved MRI and radiotherapy, recent studies have synthesized crystalline nanoparticles, polymeric micelles or functionalized different types of nanoparticles with Gd chelates or ions.[59,60]

Gd-based radiosensitization has classically been demonstrated by Gd(II) texaphyrin (Gd-tex), a porphyrin-like macrocycle that forms highly stable complexes with metal cations.[61] Gd-tex has been shown to be well tolerated in a Phase-1 single-dose trial and has been investigated as a radiotherapy adjuvant in later phase trials for advanced solid malignancies of the brain, lung and prostate.[62] A number of Gd-based nanoparticle platforms have demonstrated potential for enhancing both MRI contrast and radiotherapy efficacy. Tokumitsu et al[63,64] have developed Gd-loaded

chitosan nanoparticles composed of Gd-DTPA and chitosan, a naturally occurring biocompatible polysaccharide, for use in Gd neutron capture therapy that utilizes γ-rays and electrons emitted from ^{157}Gd (n,γ) ^{158}Gd decay. These particles have shown high cell affinity *in vitro* and significant tumour growth delay by neutron capture reaction when delivered by intratumoral injection in mice bearing B16F10 malignant melanoma tumours.

Tillement and co-workers[59] have developed the AGuIX® nanoparticle platform consisting of sub-5 nm Gd chelates (either diethylenetriaminepenta-acetate or 1,4,7,10-tetra-azacyclododecane-1-glutaric acid-4,7,10-triacetic acid covalently bonded a polysiloxane matrix) (Figure 3). Pre-clinical studies have demonstrated tolerability and excellent biodistribution patterns for diagnostic and therapeutic purposes.[59] These findings have been accompanied with demonstrations of radiosensitizing effects with DEFs from 1.1 to 2.5 in a range of tumour models including the prostate.[16,60]

These experimental studies demonstrating Gd as a radiation sensitizer are further supported by a recent Monte Carlo simulation study. Zhang et al[65] calculated DEFs as a function of Gd concentration for 6-MV photons with and without the use of a flattening filter and for HDR BT with an iridium-192 source. The study predicted concentration-dependent dose enhancement for Gd-containing materials in HDR BT and 6-MV flattening filter-free EBRT at concentrations >5 mg ml^{-1}, higher than those currently used in the clinic.

Gold-based nanoparticles

Few inorganic core materials have attracted as much attention as Au, an effect largely owing to its physical characteristics that include biocompatibility, ease of production, functionalization, large surface area and superior mass energy absorption owing to its high atomic number relative to soft tissue. The latter property warrants the development of Au-based nanoparticles (AuNPs) as effective X-ray contrast agents. Diagnostic X-ray imaging is

Figure 3. Summary of the physicochemical properties of the AGuIX® nanoparticle platform. (a) Schematic representation of AGuIX nanoparticles. The particles display a high Gd content (15%wt) with an average molecular mass of 8.7 kDa and a sub-5 nm size. (b) The hydrodynamic diameter distribution of AGuIX particles determined by dynamic light scattering indicating an average size of 3 nm. (c) Electrospray ionization mass spectrometry measurements of AGuIX particles recorded on a global spectrum. The inset indicates the spectrum generated after deconvolution with a multiplicative correlation algorithm. (d) Temporal evolution of the longitudinal relaxation (r1) for various concentrations of AGuIX particles related to their stability in human serum. Data were fitted to a monoexponential decay model.

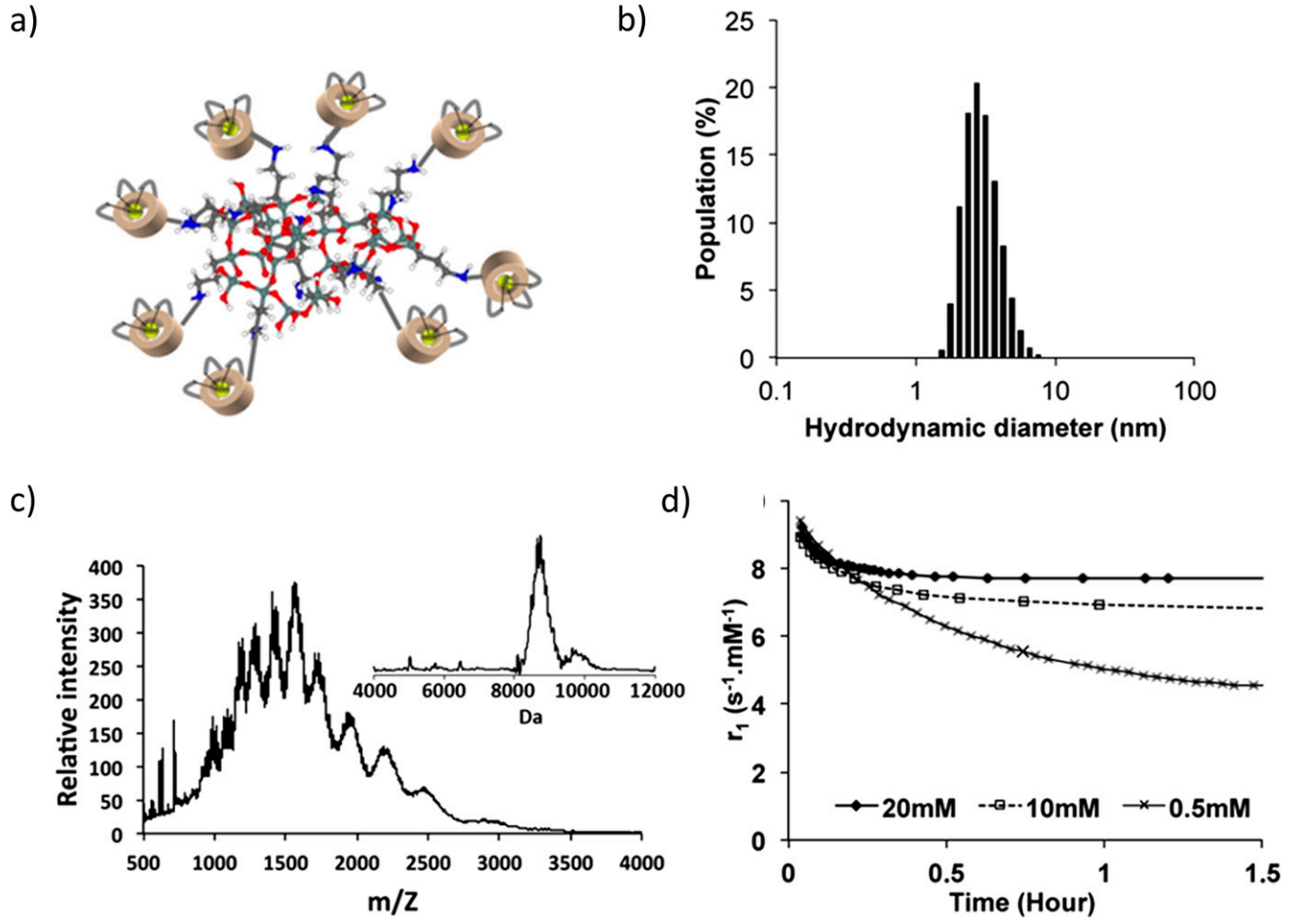

typically performed at energies <200 keV, with the Compton and photoelectric effect dominating photon absorption. Using 100-keV X-rays, Au will provide approximately 2.7-fold more contrast than iodine (I) ($Au = 5.16\,cm^2\,g^{-1}$; $I = 1.94\,cm^2\,g^{-1}$), the most commonly utilized X-ray contrast agent.[66] The first use of AuNPs to improve image contrast was reported by Hainfeld et al,[9] who described increased delineation of the vasculature, reduced bone interference and extended imaging times with no adverse events up to 1 month post administration. Since then, the list of potential targets and applications has grown exponentially with 42% of all nanoparticle publications (total 330,000 articles) since 2010 including Au within the article field. As with other nanoparticle preparations, surface modifications have been refined to improve targeting and therapeutic efficacy. Gastrin-releasing peptide receptors are highly expressed on various tumour types, including breast and prostate carcinomas, and exhibit a high binding affinity towards bombesin (BBN) peptides. Chanda et al[67] developed BBN conjugated AuNPs to specifically improve image contrast of prostate tumours. *In vitro* assessment of AuNP-BBN receptor binding using radioiodinated displacement assays demonstrated gastrin-releasing peptide receptor specificity, with IC_{50} (minimum $2.45\,\mu g\,ml^{-1}$) concentrations inversely correlated with AuNP surface coverage of the peptide. Furthermore, intraperitoneal administration of the nano-conjugate was shown to limit the uptake by the reticuloendothelial compartment, thereby extending the circulation time and tumour accumulation. This resulted in a significant and prolonged (up to 48 h) post-administration increase in X-ray contrast, highlighting the potential benefit of molecular targeted nanotherapeutics.

As described previously, PSMA is an attractive target for CaP molecular therapeutics. AuNPs functionalized with doxorubicin-loaded aptamers have been developed for both diagnostic and therapeutic applications. LNCaP cells expressing the PSMA receptor exhibited a 4-fold increase in CT intensity (Hounsfield units: LNCaP-130 HU *vs* PC3-28 HU) relative to PC3 cells lacking PSMA receptors. In addition, therapeutic efficacy of drug-loaded nanoparticles was reported to produce equivalent reductions in cell viability in PSMA-expressing cells as equimolar quantities of free doxorubicin.[68] Recently, the high electron dense properties of Au have been exploited to develop a superior radio-opaque fiducial tissue marker. In this instance, PEGylated AuNPs were combined with sucrose acetate isobutyrate to form a nanogel. Evaluated using an MRI murine model, the AuNP nanogel produced high CT contrast and excellent stability. The biocompatibility of this fiducial system was also demonstrated with no evidence of cytokine (interferon-γ, interleukin-6, or tumour necrosis factor α) stimulation associated with an innate immune cell response over a 12-week period.

Early evidence of therapeutic benefit attributed tumour growth inhibition to alternations in cell cycle regulation.[69] Glucose-capped AuNPs were avidly endocytosed into DU145 CaP cells exhibiting no significant cytotoxicity as a monotherapy. However, when combined with a 2-Gy dose of radiation (Cs137 γ-source), survival was reduced by 64% as compared with radiation alone. Radiosensitization was credited to an accelerated G0/G1 phase along with cell-cycle arrest in the more radiosensitive G2/M phase, effects driven by a reduction in p53 and cyclin A, key regulators of the cell cycle. With several groups reporting convincing *in vitro* AuNP radiosensitization,[23,39,69–71] the challenge of translating this application into effective clinical agents remains. Shukla et al[72] developed β-emitting (β_{max}, 0.96 MeV; $t_{1/2}$, 2.7 days) radioactive AuNPs conjugated with epigallocatechin-gallate (EGCg), a phytochemical component extracted from green tea that exhibits a high binding efficiency for the laminin receptor (Lam 67R), overexpressed on many prostate tumours. The ^{198}AuNP-EGCg nanoparticle was designed for direct intratumoral injection, with the targeting ligand promoting endocytosis within the tumour, while limiting passive loss of the particles into the systemic circulation. This is central to the clinical applicability of this strategy, as the β-particle emission has a tissue penetration range of 11 mm, which would likely induce dose-limiting toxicity if distributed within the systemic circulation. Following a comprehensive pharmacokinetic and tumour retention study, 70% of the total injected dose was retained within the tumour 24 h post administration, with minimal leakage into non-target organs and the blood. Furthermore, potent therapeutic efficacy was reported using a PC3 unilateral flank xenograft model. A single intratumoral injection of ^{198}AuNP-EGCg (approximately 5 MBq) supressed tumour growth by 4-fold on Day 18 compared with control animals (untreated and EGCg only), an effect that was maintained for a 5-week period. Upon sacrifice, 37.4% of the injected dose was retained within the tumour, with no treatment-associated reduction in the white blood cell compartment, nor any dose-limiting accumulations of ^{198}AuNP-EGCg in peripheral organs. Despite the relative success of this strategy, non-target radiation damage remains a significant concern that requires further pre-clinical evaluation. For localized CaP, MRI targeted, transperineal, direct intratumoral injection under local anaesthetic is feasible.

Pre-clinical studies have investigated combining AuNPs with commonly used BT sources, a concept supported by several theoretical studies.[25,26] Ngwa et al[40] reported the first experimental evidence in support of this strategy. In this *in vitro* model, HeLa cells were exposed to ^{125}I BT seeds and $200\,\mu g\,ml^{-1}$ AuNPs, with residual DNA double strand lesions used as a surrogate of potentially lethal DNA damage. Residual DNA DEFs in the presence of AuNPs ranged from 1.7 to 2.3, varying slightly as a consequence of dose rate and/or total dose administered.[73] The primary limitation of this strategy, particularly with reference to solid tumours including prostate tumours that frequently exhibit poorly vascularized cores, is achieving sufficient continual nanoparticle delivery to achieve therapeutic gain. BT spacers are routinely used in the clinic to improve spatial accuracy during seed implantation. Spacers manufactured from slow release polymers such as poly(lactic-co-glycolic acid) could be loaded with AuNPs, providing an ideal platform for prolonged continual nanoparticle release localized to the tumour. The potential therapeutic applicability of this approach has been modelled with a complex variety of parameters influencing potential dose enhancement. These include AuNP size, distance from a source, time from implantation, degradation rate of the polymer and activity/half-life of the BT seeds.[40] Although this modelling study presents the potential for therapeutic efficacy, the lack of adequate control over these variables will limit translation into the clinic.

Despite the presence of multiple *in vitro* studies demonstrating AuNP radiosensitization, there is very little *in vivo* pre-clinical evidence supporting their use in CaP treatment. At the time of writing, to the authors' knowledge, only one group has published *in vivo* efficacy. Wolfe et al[73] developed targeted Au nanorods (AuNRs), conjugated with bifunctionalized PEG chains terminated with a zwitterionic goserelin peptide. Tumours were actively targeted using goserelin, a synthetic analogue of luteinizing hormone-releasing hormone (LHRH) that binds with high affinity to the LHRH receptors overexpressed on prostate tumours.[74] Further increasing the clinical relevance of this study, radiation treatments were delivered using 6-MV X-rays. Goserelin-targeted AuNRs conferred a significant dose enhancement of 1.32 over radiation only and 17% increase over the unfunctionalized nanoparticle. The importance of this differential between targeted and untargeted AuNRs was further heightened *in vivo*. Radiosensitization efficacy, defined by delay in the time for subcutaneous PC3 tumours to triple in volume, was extended by 17 ± 1 day in the goserelin-targeted AuNR treatment group compared with radiation only, whereas the untargeted AuNRs accumulating by passive targeting only (EPR) produced no significant delay in tumour growth over radiation only. Furthermore, no significant treatment-related adverse events were reported.[73] Owing to the relative simplicity, lack of toxicity and therapeutic efficacy of this approach, considered in tandem with the frequency of use of external EBRT in CaP, this strategy appears to represent the most likely translation of nanoparticles into regular clinical use.

CONCLUSIONS

The radiotherapeutic management of CaP is rapidly changing with IG-IMRT now the standard of care, increasing evidence for combination strategies with BT and ADT and the emerging role of MRI, dose-painting and adaptive treatment strategies. In parallel, rapid advances in metal nanoparticle synthesis, targeting and manufacture are occurring. The integration of these exciting advances should enable improvement in the management of CaP in the years to come.

REFERENCES

1. Cancerresearchuk.org. London, UK: Cancer Research UK. [Cited 20 March 2015.] Available from: http://www.cancerresearchuk.org/cancer-info/cancerstats/types/prostate/mortality/uk-prostate-cancer-mortality-statistics.
2. Lagendijk JJ, Raaymakers BW, van Vulpen M. The magnetic resonance imaging-linac system. *Semin Radiat Oncol* 2014; **24**: 207–9. doi: 10.1016/j.semradonc.2014.02.009
3. Keall PJ, Barton M, Crozier S; Australian MRI-Linac Program, including contributors from Ingham Institute, Illawarra Cancer Care Centre, Liverpool Hospital, Stanford University, Universities of Newcastle, Queensland, Sydney, Western Sydney, and Wollongong. The Australian magnetic resonance imaging-linac program. *Semin Radiat Oncol* 2014; **24**: 203–6. doi: 10.1016/j.semradonc.2014.02.015
4. Jaffray DA, Carlone MC, Milosevic MF, Breen SL, Stanescu T, Rink A, et al. A facility for magnetic resonance-guided radiation therapy. *Semin Radiat Oncol* 2014; **24**: 193–5. doi: 10.1016/j.semradonc.2014.02.012
5. Wei H, Rodriguez K, Renneckarbd S, Vikesland PJ. Environmental science and engineering applications of nanocellulose-based nanocomposites. *Environ Sci Nano* 2014; **1**: 302–16.
6. Zhong Y, Zhang J, Cheng R, Deng C, Meng F, Xie F, et al. Reversibly crosslinked hyaluronic acid nanoparticles for active targeting and intelligent delivery of doxorubicin to drug resistant CD44+ human breast tumor xenografts. *J Control Release* 2015; **205**: 144–54. doi: 10.1016/j.jconrel.2015.01.012
7. Peng LH, Niu J, Zhang CZ, Yu W, Wu JH, Shan YH, et al. TAT conjugated cationic noble metal nanoparticles for gene delivery to epidermal stem cells. *Biomaterials* 2014; **35**: 5605–18. doi: 10.1016/j.biomaterials.2014.03.062
8. Howes PD, Chandrawati R, Stevens MM. Bionanotechnology. Colloidal nanoparticles as advanced biological sensors. *Science* 2014; **346**: 1247390. doi: 10.1126/science.1247390
9. Hainfeld JF, Slatkin DN, Focella TM, Smilowitz HM. Gold nanoparticles: a new X-ray contrast agent. *Br J Radiol* 2006; **79**: 248–53. doi: 10.1259/bjr/13169882
10. Ren F, Bhana S, Norman DD, Johnson J, Xu L, Baker DL, et al. Gold nanorods carrying paclitaxel for photothermal-chemotherapy of cancer. *Bioconjug Chem* 2013; **24**: 376–86. doi: 10.1021/bc300442d
11. Jain S, Coulter JA, Hounsell AR, Butterworth KT, McMahon SJ, Hyland WB, et al. Cell-specific radiosensitization by gold nanoparticles at megavoltage radiation energies. *Int J Radiat Oncol Biol Phys* 2011; **79**: 531–9. doi: 10.1016/j.ijrobp.2010.08.044
12. Dearnaley DP, Jovic G, Syndikus I, Khoo, V. Cowan, RA, Graham JD, et al. Escalated-dose *versus* control-dose conformal radiotherapy for prostate cancer: long-term results from the MRC RT01 randomised controlled trial. *Lancet Oncol* 2014; **15**: 464–73. doi: 10.1016/S1470-2045(14)70040-3
13. Klotz L. Active surveillance for prostate cancer: for whom? *J Clin Oncol* 2005; **23**: 8165–9. doi: 10.1200/JCO.2005.03.3134
14. Klotz L, Vesprini D, Sethukavalan P, Jethava V, Zhang L, Jain S, et al. Long-term follow-up of a large active surveillance cohort of patients with prostate cancer. *J Clin Oncol* 2015; **33**: 272–7. doi: 10.1200/JCO.2014.55.1192
15. Jain S, Loblaw A, Vesprini D, Zhang L, Kattan MW, Mamedov A, et al. Gleason upgrading with time in a large prostate cancer active surveillance cohort. *J Urol* 2015; in press. doi: 10.1016/j.juro.2015.01.102
16. Lux F, Sancey L, Bianchi A, Crémillieux Y, Roux S, Tillement O. Gadolinium-based nanoparticles for theranostic MRI-radiosensitization. *Nanomedicine (Lond)* Feb 2015: 1–15. Epub ahead of print. doi: 10.2217/nnm.15.30
17. van As NJ, de Souza NM, Riches SF, Morgan VA, Sohaib SA, Dearnaley DP, et al. A study of diffusion-weighted magnetic resonance imaging in men with untreated localised prostate cancer on active surveillance. *Eur Urol* 2009; **56**: 981–8. doi: 10.1016/j.eururo.2008.11.051
18. Harisinghani MG, Barentsz J, Hahn PF, Deserno WM, Tabatabaei S, van de Kaa CH, et al. Noninvasive detection of clinically occult lymph-node metastases in prostate cancer. *N Engl J Med* 2003; **348**: 2491–9. doi: 10.1056/NEJMoa022749
19. Pollack A, Zagars GK, Smith LG, Lee JJ, von Eschenbach AC, Antolak JA, et al. Preliminary results of a randomized radiotherapy dose-escalation study comparing 70 Gy with 78 Gy for prostate cancer. *J Clin Oncol* 2000; **18**: 3904–11.
20. Zietman AL, Desilvio ML, Slater JD, Rossi CJ Jr, Miller DW, Adams JA, et al.

Comparison of conventional-dose *vs* high-dose conformal radiation therapy in clinically localized adenocarcinoma of the prostate: a randomized controlled trial. *JAMA* 2005; **294**: 1233–9.

21. Peeters ST, Heemsbergen WD, Koper PC, van Putten WL, Slot A, Dielwart MF, et al. Dose-response in radiotherapy for localized prostate cancer: results of the Dutch multicenter randomized phase III trial comparing 68 Gy of radiotherapy with 78 Gy. *J Clin Oncol* 2006; **24**: 1990–6. doi: 10.1200/JCO.2005.05.2530
22. Dearnaley DP, Sydes MR, Graham JD, Aird EG, Bottomley D, Cowan RA, et al. Escalated-dose *versus* standard-dose conformal radiotherapy in prostate cancer: first results from the MRC RT01 randomised controlled trial. *Lancet Oncol* 2007; **8**: 475–87.
23. Chithrani DB, Jelveh S, Jalali F, van Prooijen M, Allen C, Bristow RG, et al. Gold nanoparticles as radiation sensitizers in cancer therapy. *Radiat Res* 2010; **173**: 719–28. doi: 10.1667/RR1984.1
24. Joiner MC, Van der Kogel AJ. *Basic clinical radiobiology*. London, UK: Hodder Arnold; 2009. pp. 173–83.
25. Cho SH, Jones BL, Krishnan S. The dosimetric feasibility of gold nanoparticle-aided radiation therapy (GNRT) *via* brachytherapy using low-energy gamma-/x-ray sources. *Phys Med Biol* 2009; **54**: 4889–905. doi: 10.1088/0031-9155/54/16/004
26. Sinha N, Cifter G, Sajo E, Kumar R, Sridhar S, Nguyen PL, et al. Brachytherapy application with in situ dose painting administered by gold nanoparticle eluters. *Int J Radiat Oncol Biol Phys* 2015; **91**: 385–92. doi: 10.1016/j.ijrobp.2014.10.001
27. Morton GC, Hoskin PJ. Brachytherapy: current status and future strategies—can high dose rate replace low dose rate and external beam radiotherapy?. *Clin Oncol (R Coll Radiol)* 2013; **25**: 474–82. doi: 10.1016/j.clon.2013.04.009
28. Helou J, D'Alimonte L, Loblaw A, Chung H, Cheung P, Szumacher E, et al. High dose-rate brachytherapy boost for intermediate risk prostate cancer: long-term outcomes of two different treatment schedules and early biochemical predictors of success. *Radiother Oncol* 2015; **115**: 84–9. doi: 10.1016/j.radonc.2015.02.023
29. Miralbell R, Roberts SA, Zubizarreta E, Hendry JH. Dose-fractionation sensitivity of prostate cancer deduced from radiotherapy outcomes of 5,969 patients in seven international institutional datasets: $\alpha/\beta = 1.4$ (0.9-2.2) Gy. *Int J Radiat Oncol Biol Phys* 2012; **82**: 17–24. doi: 10.1016/j.ijrobp.2010.10.075
30. Loblaw A, Cheung P, D'alimonte L, Deabreu A, Mamedov A, Zhang L, et al. Prostate stereotactic ablative body radiotherapy using a standard linear accelerator: toxicity, biochemical, and pathological outcomes. *Radiother Oncol* 2013; **107**: 153–8. doi: 10.1016/j.radonc.2013.03.022
31. Tree AC, Ostler P, Hoskin P, Dankulchai P, Nariyangadu P, Hughes RJ, et al. Prostate stereotactic body radiotherapy—first UK experience. *Clin Oncol (R Coll Radiol)* 2014; **26**: 757–61. doi: 10.1016/j.clon.2014.08.007
32. Bolla M, Collette L, Blank L, Warde P, Dubois JB, Mirimanoff RO, et al. Long-term results with immediate androgen suppression and external irradiation in patients with locally advanced prostate cancer (an EORTC study): a phase III randomised trial. *Lancet* 2002; **36**: 103–6.
33. Mason MD, Parulekar WR, Sydes MR, Brundage M, Kirkbride P, Gospodarowicz M, et al. Final report of the intergroup randomized study of combined androgen-deprivation therapy plus radiotherapy *versus* androgen-deprivation therapy alone in locally advanced prostate cancer. *J Clin Oncol* 2015; in press. Epub ahead of print. doi: JCO.2014.57.7510
34. Libutti SK, Paciotti GF, Byrnes AA, Alexander HR Jr, Gannon WE, Walker M, et al. Phase I and pharmacokinetic studies of CYT-6091, a novel PEGylated colloidal gold-rhTNF nanomedicine. *Clin Cancer Res* 2010; **16**: 6139–49. doi: 10.1158/1078-0432.CCR-10-0978
35. Bhattacharya IS, Woolf DK, Hughes RJ, Shah N, Harrison N, Ostler PJ, et al. Stereotactic body radiotherapy (SBRT) in the management of extracranial oligometastatic (OM) disease. *Br J Radiol* 2015; **88**: 20140712. doi: 10.1259/bjr.20140712
36. Parker C, Nilsson S, Heinrich D, Helle SI, O'Sullivan JM, Fosså SD, et al; ALSYMPCA Investigators. Alpha emitter radium-223 and survival in metastatic prostate cancer. *N Engl J Med* 2013; **369**: 213–23. doi: 10.1056/NEJMoa1213755
37. Daniel MC, Astruc D. Gold nanoparticles: assembly, supramolecular chemistry, quantum-size-related properties, and applications toward biology, catalysis, and nanotechnology. *Chem Reviews*. 2004; **104**: 293–346.
38. Ghosh A, Heston WD. Tumor target prostate specific membrane antigen (PSMA) and its regulation in prostate cancer. *J Cell Biochem* 2004; **91**: 528–39.
39. Zhang X, Xing JZ, Chen J, Ko L, Amanie J, Gulavita S, et al. Enhanced radiation sensitivity in prostate cancer by gold-nanoparticles. *Clin Invest Med* 2008; **31**: E160–7.
40. Ngwa W, Korideck H, Kassis AI, Kumar R, Sridhar S, Makrigiorgos GM, et al. *In vitro* radiosensitization by gold nanoparticles during continuous low-dose-rate gamma irradiation with I-125 brachytherapy seeds. *Nanomedicine* 2013; **9**: 25–7. doi: 10.1016/j.nano.2012.09.001
41. Babincová M, Babinec P, Bergemann C. High-gradient magnetic capture of ferrofluids: implications for drug targeting and tumor embolization. *Z Naturforsch C* 2001; **56**: 909–11.
42. Schmittgen TD, Teske S, Vessella RL, True LD, Zakrajsek BA. Expression of prostate specific membrane antigen and three alternatively spliced variants of PSMA in prostate cancer patients. *Int J Cancer* 2003; **107**: 323–9. doi: 10.1002/ijc.11402
43. Bates D, Abraham S, Campbell M, Zehbe I, Curiel L. Development and characterization of an antibody-labeled super-paramagnetic iron oxide contrast agent targeting prostate cancer cells for magnetic resonance imaging. *PLoS One* 2014; **9**: e97220. doi: 10.1371/journal.pone.0097220
44. Wright GL Jr, Grob BM, Haley C, Grossman K, Newhall K, Petrylak D, et al. Upregulation of prostate-specific membrane antigen after androgen-deprivation therapy. *Urology* 1996; **48**: 326–34.
45. Tse BW, Cowin GJ, Soekmadji C, Jovanovic L, Vasireddy RS, Ling MT, et al. PSMA-targeting iron oxide magnetic nanoparticles enhance MRI of preclinical prostate cancer. *Nanomedicine (Lond)* 2015; **10**: 375–86. doi: 10.2217/nnm.14.122
46. Vallabhajosula S, Kuji I, Hamacher KA, Konishi S, Kostakoglu L, Kothari PA, et al. Pharmacokinetics and biodistribution of 111In- and 177Lu-labeled J591 antibody specific for prostate-specific membrane antigen: prediction of 90Y-J591 radiation dosimetry based on 111In or 177Lu? *J Nucl Med* 2005; **46**: 634–41.
47. Bander NH, Milowsky MI, Nanus DM, Kostakoglu L, Vallabhajosula S, Goldsmith SJ. Phase I trial of 177lutetium-labeled J591, a monoclonal antibody to prostate-specific membrane antigen, in patients with androgen-independent prostate cancer. *J Clin Oncol* 2005; **23**: 4591–601.
48. Banerjee SR, Foss CA, Castanares M, Mease RC, Byun Y, Fox JJ, et al. Synthesis and evaluation of technetium-99m- and rhenium-labeled inhibitors of the prostate-specific membrane antigen (PSMA). *J Med Chem* 2008; **51**: 4504–17. doi: 10.1021/jm800111u
49. Behnam Azad B, Banerjee SR, Pullambhatla M, Lacerda S, Foss CA, Wang Y, et al.

Evaluation of a PSMA-targeted BNF nanoparticle construct. *Nanoscale* 2015; **7**: 4432–42. doi: 10.1039/c4nr06069e
50. Eggeman AS, Majetich SA, Farrell D, Pankhurst QA. Size and concentration effects on high frequency hysteresis of iron oxide nanoparticles. *IEEE Trans Magn* 2007; **43**: 2451–3.
51. Dennis CL, Jackson AJ, Borchers JA, Hoopes PJ, Strawbridge R, Foreman AR, et al. Nearly complete regression of tumors *via* collective behavior of magnetic nanoparticles in hyperthermia. *Nanotechnology* 2009; **20**: 395103. doi: 10.1088/0957-4484/20/39/395103
52. Ivkov R, DeNardo SJ, Daum W, Foreman AR, Goldstein RC, Nemkov VS, et al. Application of high amplitude alternating magnetic fields for heat induction of nanoparticles localized in cancer. *Clin Cancer Res* 2005; **11**: 7093s–103s. doi: 10.1158/1078-0432.CCR-1004-0016
53. Huang FK, Chen WC, Lai SF, Liu CJ, Wang CL, Wang CH, et al. Enhancement of irradiation effects on cancer cells by cross-linked dextran-coated iron oxide (CLIO) nanoparticles. *Phys Med Biol* 2010; **55**: 469–82. doi: 10.1088/0031-9155/55/2/009
54. Khoei S, Mahdavi SR, Fakhimikabir H, Shakeri-Zadeh A, Hashemian A. The role of iron oxide nanoparticles in the radiosensitization of human prostate carcinoma cell line DU145 at megavoltage radiation energies. *Int J Radiat Biol* 2014; **90**: 351–6. doi: 10.3109/09553002.2014.888104
55. Na H, Song I, Hyeon T. Inorganic nanoparticles for MRI contrast agents. *Adv Mater* 2009; **21**: 2133–48.
56. Jung CW, Jacobs P. Physical and chemical properties of superparamagnetic iron oxide MR contrast agents: ferumoxides, ferumoxtran, ferumoxsil. *Magn Reson Imaging* 1995; **13**: 661–74.
57. Rosen BR, Belliveau JW, Vevea JM, Brady TJ. Perfusion imaging with NMR contrast agents. *Magn Reson Med* 1990; **14**: 249–65.
58. Erlemann R, Reiser MF, Peters PE, Vasallo P, Nommensen B, Kusnierz-Glaz CR, et al. Musculoskeletal neoplasms: static and dynamic Gd-DTPA–enhanced MR imaging. *Radiology* 1989; **171**: 767–73.
59. Sancey L, Lux F, Kotb S, Roux S, Dufort S, Bianchi A, et al. The use of theranostic gadolinium-based nanoprobes to improve radiotherapy efficacy. *Br J Radiol* 2014; **87**: 20140134. doi: 10.1259/bjr.20140134
60. Sancey L, Kotb S, Truillet C, Appaix F, Marais A, Thomas E, et al. Long-term *in vivo* clearance of gadolinium-based AGuIX nanoparticles and their biocompatibility after systemic injection. *ACS Nano* 2015; **9**: 2477–88. doi: 10.1021/acsnano.5b00552
61. Young SW, Qing F, Harriman A, Sessler JL, Dow WC, Mody TD, et al. Gadolinium(III) texaphyrin: a tumor selective radiation sensitizer that is detectable by MRI. *Proc Natl Acad Sci U S A* 1996; **93**: 6610–15.
62. Rosenthal DI, Nurenberg P, Becerra CR, Frenkel EP, Carbone DP, Lum BL, et al. A phase I single-dose trial of gadolinium texaphyrin (Gd-Tex), a tumor selective radiation sensitizer detectable by magnetic resonance imaging. *Clin Cancer Res* 1999; **5**: 739–45.
63. Shikata F, Tokumitsu H, Ichikawa H, Fukumori Y. *In vitro* cellular accumulation of gadolinium incorporated into chitosan nanoparticles designed for neutron-capture therapy of cancer. *Eur J Pharm Biopharm* 2002; **53**: 57–63.
64. Tokumitsu H, Hiratsuka J, Sakurai Y, Kobayashi T, Ichikawa H, Fukumori Y. Gadolinium neutron-capture therapy using novel gadopentetic acid-chitosan complex nanoparticles: *in vivo* growth suppression of experimental melanoma solid tumor. *Cancer Lett* 2000; **150**: 177–82.
65. Zhang DG, Feygelman V, Moros EG, Latifi K, Zhang GG. Monte Carlo study of radiation dose enhancement by gadolinium in megavoltage and high dose rate radiotherapy. *PLoS One* 2014; **9**: e109389. doi: 10.1371/journal.pone.0109389
66. Hubbell JH, Seltzer SM. *Tables of X-ray mass attenuation coefficients and mass energy-absorption coefficients from 1 keV to 20MeV for elements Z=1 to 92 and 48 additional substances of dosimetric interest*. Gaithersburg, MD: National Institute of Standards and Technology, US Department of Commerce; 1996.
67. Chanda N, Kattumuri V, Shukla R, Zambre A, Katti K, Upendran A, et al. Bombesin functionalized gold nanoparticles show *in vitro* and *in vivo* cancer receptor specificity. *Proc Natl Acad Sci U S A* 2010; **107**: 8760–5. doi: 10.1073/pnas.1002143107
68. Kim D, Jeong YY, Jon S. A drug-loaded aptamer-gold nanoparticle bioconjugate for combined CT imaging and therapy of prostate cancer. *ACS Nano* 2010; **4**: 3689–96. doi: 10.1021/nn901877h
69. Roa W, Zhang X, Guo L, Shaw A, Hu X, Xiong Y, et al. Gold nanoparticle sensitize radiotherapy of prostate cancer cells by regulation of the cell cycle. *Nanotechnology* 2009; **20**: 375101. doi: 10.1088/0957-4484/20/37/375101
70. Kong T, Zeng J, Wang X, Yang X, Yang J, McQuarrie S, et al. Enhancement of radiation cytotoxicity in breast-cancer cells by localized attachment of gold nanoparticles. *Small* 2008; **4**: 1537–43. doi: 10.1002/smll.200700794
71. Butterworth KT, Coulter JA, Jain S, Forker J, McMahon SJ, Schettino G, et al. Evaluation of cytotoxicity and radiation enhancement using 1.9 nm gold particles: potential application for cancer therapy. *Nanotechnology* 2010; **21**: 295101. doi: 10.1088/0957-4484/21/29/295101
72. Shukla R, Chanda N, Zambre A, Upendran A, Katti K, Kulkarni RR, et al. Laminin receptor specific therapeutic gold nanoparticles (198AuNP-EGCg) show efficacy in treating prostate cancer. *Proc Natl Acad Sci U S A* 2012; **109**: 12426–31. doi: 10.1073/pnas.1121174109
73. Wolfe T, Chatterjee D, Lee J, Grant JD, Bhattarai S, Tailor R, et al. Targeted gold nanoparticles enhance sensitization of prostate tumors to megavoltage radiation therapy *in vivo*. *Nanomedicine* 2015; **11**: 1277–83. doi: 10.1016/j.nano.2014.12.016
74. Halmos G, Arencibia JM, Schally AV, Davis R, Bostwick DG. High incidence of receptors for luteinizing hormone-releasing hormone (LHRH) and LHRH receptor gene expression in human prostate cancers. *J Urol* 2000; **163**: 623–9.